Electronic Supporting Information (ESI)

Concentration-Dependent Nucleation of Pyrazinamide Polymorphs Monitored by Dynamic Light Scattering

Sakshi P. Dahake,[a] Manish Kumar Mishra,[b,c] and Kamini Mishra[a,*]

[a]Department of Chemistry, School of Advanced Sciences, Vellore Institute of Technology, Vellore 632014, Tamil Nadu, India

[b]Physical and Materials Chemistry Division, CSIR-National Chemical Laboratory, Pune 411008, India

[c]Academy of Scientific and Innovative Research (AcSIR), Ghaziabad, Uttar Pradesh 201002, India

Control Experiment:

In our experiments, all the solutions were filtered using 0.2 μm pore-size syringe filters, the membrane was selected depending on solvent compatibility. For water and methanol, we used Acrodisc Supor syringe filters with 0.2 μm polyethersulfone (PES) membranes. PES is a hydrophilic material suitable for aqueous media, buffers, biological solutions, and low-molecular-weight alcohols such as methanol. However, PES membranes are not compatible with higher alcohols or other organic solvents, where membrane swelling can occur. Therefore, for ethanol, acetone, THF, we used 0.2 μm PVDF syringe filters, which are compatible with organic solvents and ensure sample integrity. The DLS control experiments were conducted with all solvents individually under identical experimental conditions.

For each solvent, the initial DLS reading was recorded after an equilibration time of 120 seconds, while subsequent measurements employed an equilibration time of 10 minutes at 25.0 °C. As a control experiment, we measured the hydrodynamic diameter of only the solvent (without PYZ), to ensure the curves obtained in nucleation experiments (with PYZ) were not any artifact due to the solvent. For the sole solvent, the instrument was unable to extract a meaningful autocorrelation function due to very low scattering intensity. Consequently, the DLS software reported stochastic, hydrodynamic diameters and displayed a warning indicating low scattering. Therefore, neither reproducible nor meaningful particle-size data could be obtained for the only solvent (without PYZ). The control experiment readings for MeOH, Ac, H_2O, THF, and EtOH were arbitrary and did not yield any reliable particle-size information. The weak and inconsistent signals detected in the control experiments arise purely from scattering noise and cannot be interpreted as representative of nucleation behavior.

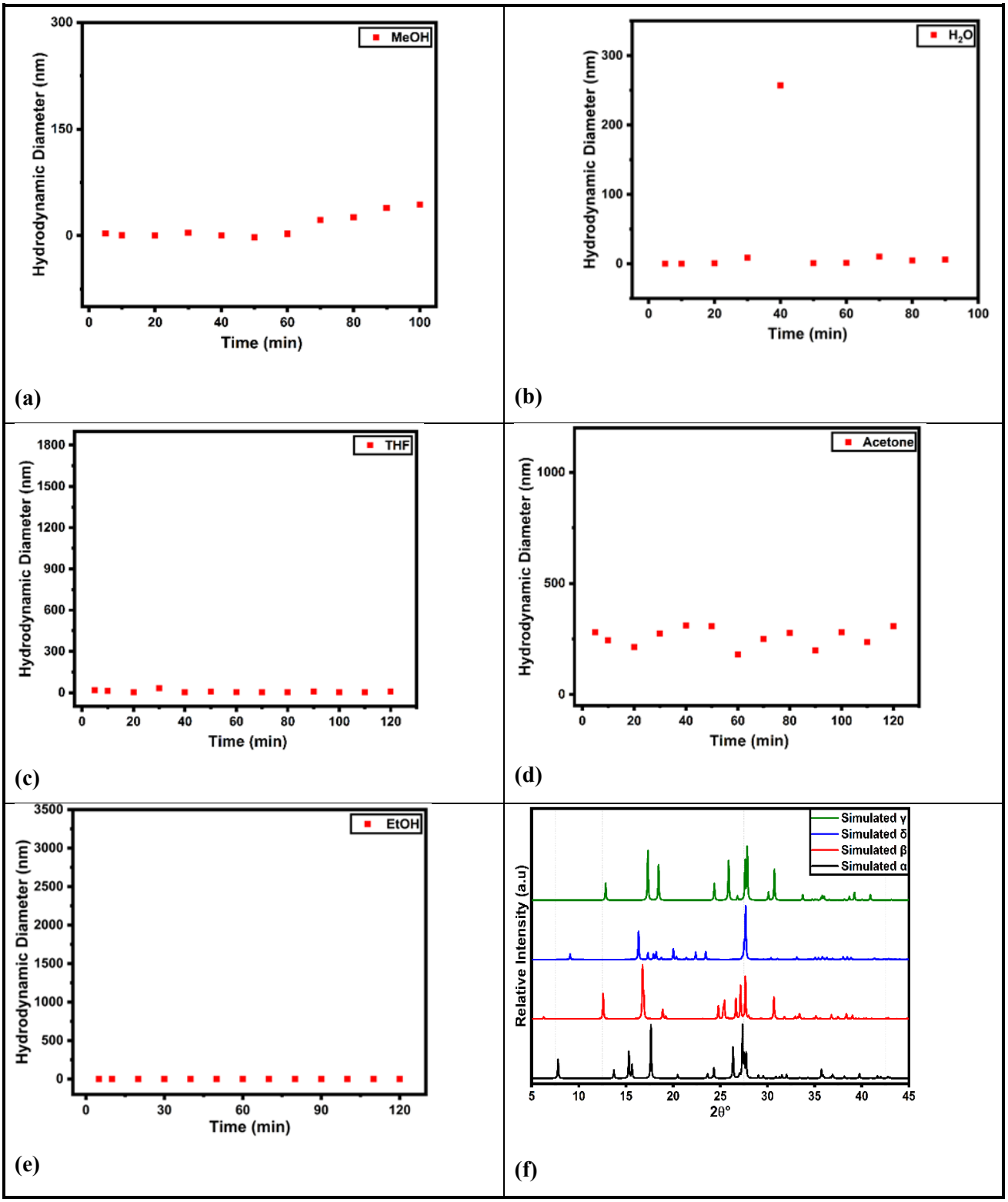

Fig.S1 DLS graph represents the control experiments for the solvents: MeOH (a), H2O (b), THF (c), acetone (d), EtOH (e) & (f) Simulated Powder X-ray diffraction (PXRD) pattern of alpha, beta, delta, gamma form.

Induction Time Experiment:

Induction time measurements were performed at various supersaturation ratios for the five solvents. For each solvent, multiple supersaturation ratios (*S*) were systematically investigated. Solutions were prepared at 318.15 K under continuous stirring to ensure complete dissolution. The solutions were then rapidly cooled to 298.15 K at an average cooling rate of 0.0554 K s^{-1} and maintained isothermally at 298.15 K. The time at which 298.15 K was reached was defined as t_o. Transmittance was continuously recorded, and the onset of nucleation was identified by a sudden, irreversible decrease in transmittance. The induction time was calculated as: $t_{ind} = t - t_o$.

According to Classical Nucleation Theory (CNT), the nucleation rate (*J*) is given by:

$$J = Aexp\left(-\frac{16\pi\gamma^3 v^2}{3(kT)^3(ln\,S)^2}\right) \quad (1)$$

where γ is the solid-liquid interfacial energy, *v* is the molecular volume, *k* is Boltzmann's constant, and T is temperature.

Taking logarithms:

$$\ln J = \ln A - \frac{16\pi\gamma^3 v^2}{3(kT)^3} \cdot \frac{1}{(\ln S)^2} \quad (2)$$

Since $J \propto 1/t_{ind}$,

$$\ln\left(\frac{1}{t_{ind}}\right) = \ln A' - \frac{16\pi\gamma^3 v^2}{3(kT)^3} \cdot \frac{1}{(\ln S)^2} \quad (3)$$

Thus, a linear relationship between $\ln(1/t_{ind})$ and $1/(\ln S)^2$ is expected. The observed linearity in the present study indicates that nucleation follows a thermodynamically controlled CNT mechanism within the investigated supersaturation range. The slope of the fitted line was used to extract γ values, and the corresponding nucleation rates (*J*) were subsequently calculated.

All solid samples recovered from the induction time experiments were analyzed by PXRD. Under the higher supersaturation conditions employed in these experiments, no competing or coexisting polymorphic phases were observed. Instead, a single polymorph was consistently obtained in each solvent system: the δ-form in THF, EtOH, MeOH, and acetone, and the α-form in water. In contrast, polymorphic transitions were observed in the concentration regime investigated in the hydrodynamic diameter (DLS) experiments. The absence of polymorphic variation in the induction experiments is likely due to the higher supersaturation levels employed, where rapid nucleation favors the kinetically accessible stable phase in the

respective solvent and limits the time available for polymorphic transformation (fig. S2).

Solvents	Supersaturation ratio (*S*)	Induction Time (t_{ind}) (s)	Interfacial energy (γ) (J/m^2)(10^{-3})	Nucleation rate (*J*) (m^{-3}s^{-1})	R^2
Water	1.80 1.90 2.20	17400 6780 2700	6.47	21.8 41 132.2	0.9735 5
THF	1.30 1.45 1.52	12840 6600 4920	2.69	25.6 54.5 61.6	0.9806 8
EtOH	2.00 2.20 2.50	11940 8760 7680	4.58	29 36.1 44.6	0.9631 6
MeOH	1.30 1.40 1.60	7800 5880 4020	2.31	41.6 60.5 80.4	0.9730 5
Acetone	1.30 1.40 1.60	6840 5220 4080	2.14	48.2 64.7 80.9	0.9971 6

Table S1. Induction time, interfacial energy, nucleation rate at different supersaturation ratio and the R-square value obtained from the linear fit.

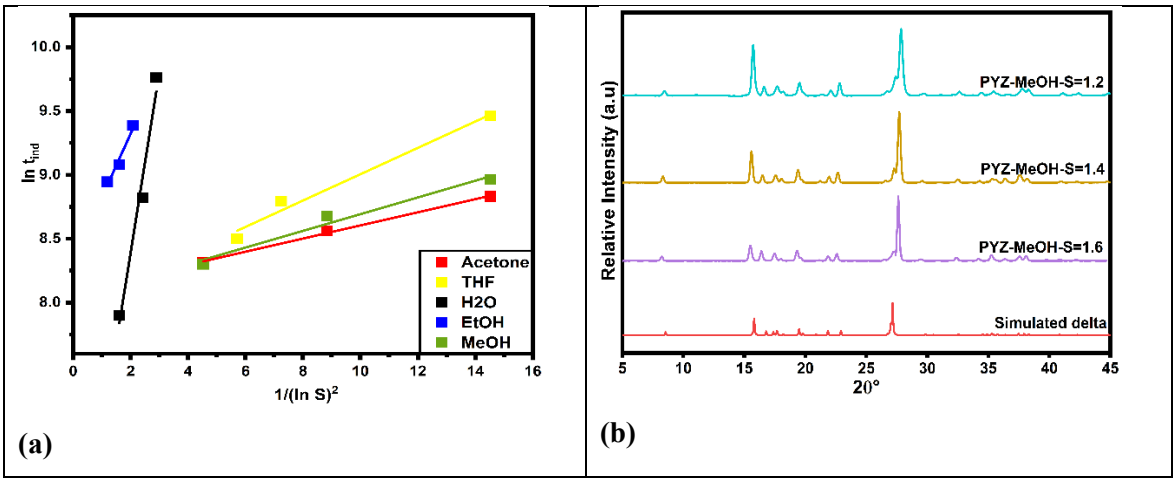

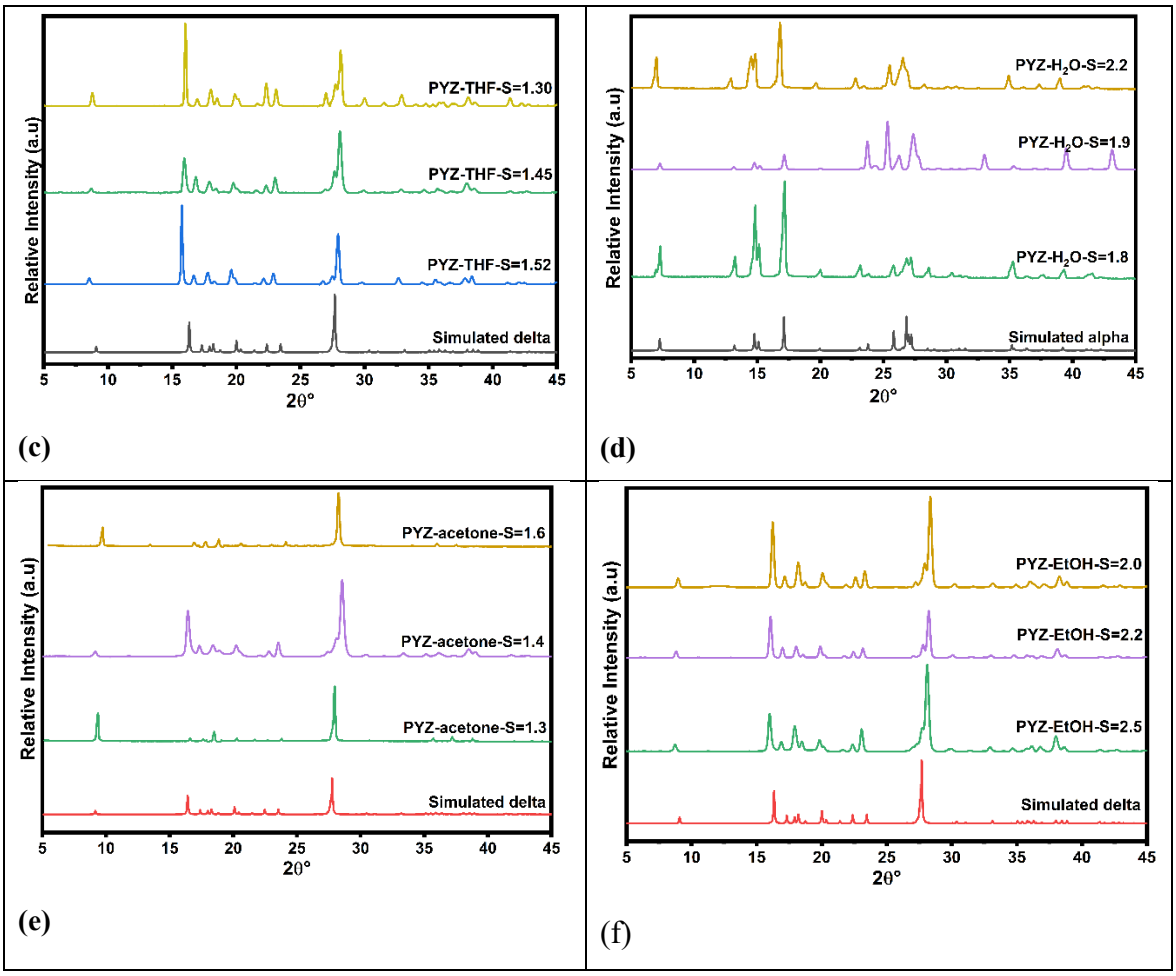

Fig. S2. (a) Dependence of the induction time, $t_{ind,}$ on the supersaturation ratio, *S*, in different solvent. Powder X-ray diffraction (PXRD) patterns of pyrazinamide crystals obtained from the induction time experiments in, (b) MeOH, (c) THF, (d) H_2O, and (e) acetone, (f) EtOH.

Relationship between solvation energy (ΔG_{sol}) and hydrodynamic diameter:

A statistical analysis was performed to validate the relationship between solvation energy and hydrodynamic diameter. To quantitatively evaluate the relationship between solvation energy and hydrodynamic diameter, a linear regression analysis was performed (Fig. S3). Linear regression yielded with $R^2 = 0.7566$ (and correlation coefficient of $R = 0.8698$), indicating a reasonably strong dependence of particle size on solvation energy. This implies that solvents with more negative solvation energies (stronger solute-solvent interactions) tend to produce smaller hydrodynamic diameters. Although the dataset is limited and exhibits some deviation from ideal linearity, the observed trend provides quantitative support for the proposed inverse relationship between solvation strength and early-stage particle size evolution.

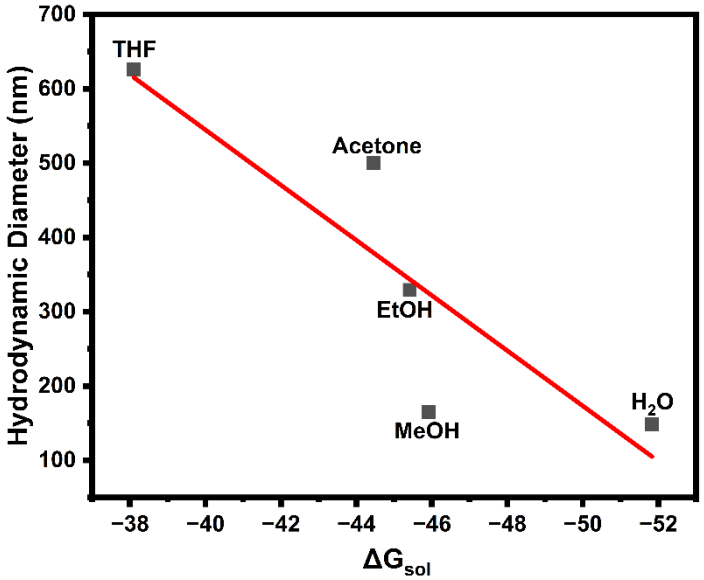

Fig. S3. Relationship between solvation energy (ΔG_{sol}) and hydrodynamic diameter at 120 min (20 mg). The solid line represents a linear regression fit ($R^2 = 0.76$).